Elucidation of the Structure of a Highly Active Catalytic System for CO2/Epoxide Copolymerization: A salen−Cobaltate Complex of an Unusual Binding Mode

ARTICLE *in* INORGANIC CHEMISTRY · SEPTEMBER 2009

Impact Factor: 4.76 · DOI: 10.1021/ic901584u · Source: PubMed

9 AUTHORS, INCLUDING:

Youn K. Kang
Sangmyung University
34 PUBLICATIONS **610** CITATIONS

SEE PROFILE

Inorganic Chemistry
Article

Inorg. Chem. **2009**, *48*, 10455–10465 **10455**
DOI: 10.1021/ic901584u

Elucidation of the Structure of a Highly Active Catalytic System for CO_2/Epoxide Copolymerization: A salen-Cobaltate Complex of an Unusual Binding Mode

Sung Jae Na,[†] Sujith S,[†] Anish Cyriac,[†] Bo Eun Kim,[†] Jina Yoo,[†] Youn K. Kang,[‡] Su Jung Han,[§] Chongmok Lee,[§] and Bun Yeoul Lee*,[†]

[†]*Department of Molecular Science and Technology, Ajou University, Suwon 443-749 Korea,* [‡]*Division of Chemistry and Molecular Engineering, Department of Chemistry, College of Natural Sciences, Seoul National University, Seoul 151-747 Korea, and* [§]*Department of Chemistry and Nano Science, Ewha Womans University, Seoul 120-750, Korea*

Received August 8, 2009

Salen-type ligands comprised of ethylenediamine or 1,2-cyclohexenediamine, along with an salicylaldehyde bearing a methyl substituent on its 3-position and a $-[CR(CH_2CH_2CH_2N^+Bu_3)_2]$ (R = H or Me) on its 5-position, unexpectedly afford cobalt(III) complexes with uncoordinated imines. In these complexes, two salen−phenoxys and two 2,4-dinitrophenolates (DNPs), which counter the quaternary ammonium cations, coordinate persistently with cobalt, while two other DNPs are fluxional between a coordinated and an uncoordinated state in THF at room temperature. The complexes of this binding mode show excellent activities in carbon dioxide/propylene oxide copolymerization (TOF, 8 300−13 000 h^{-1}) but with some fluctuation in induction times (1−10 h), depending on how dry the system is. The induction time is shortened (<1.0 h) and activity is increased ∼1.5 times upon the replacement of the two fluxional DNPs with 2,4-dinitrophenol-2,4-dinitrophenolate homoconjugation ($[DNP\cdots H\cdots DNP]^-$). Imposing steric congestion either by replacing the methyl substituent on the salicylaldehyde with *tert*-butyl or by employing H_2NCMe_2C-Me_2NH_2 instead of ethylenediamine or 1,2-cyclohexenediamine results in conventional imine-coordinating complexes, which show lower activities than uncoordinated imine complexes.

Introduction

The carbon dioxide/propylene oxide (CO_2/PO) copolymer has attracted much interest due to its favorable properties.[1] The copolymer, which consists of alternating CO_2 and PO subunits, is composed of 44% CO_2 by weight, making the copolymer economical to prepare due to the abundance and the cheapness of CO_2 gas. The copolymer burns gently in air without emitting toxic materials, decomposes at the relatively low temperature of approximately 250 °C without producing an ash residue, and adheres strongly to a cellulosic substrate. We recently reported a highly active catalyst (**3** in eq 1) with the potential to be commercially applied.[2] The success of this would require the binding of two components or two metal centers in proximity, regardless of low catalyst concentration or high polymerization temperature, resulting in a high turnover number (TON) and a high molecular weight (M_n) of the resulting polymers.[3] However, conventional binary systems of [(salen)Co[4] or (salen)Cr complex[5]]/(onium salt or base), in which the two components are not bound, suffer low catalytic performance at low catalyst concentrations and/or high polymerization temperatures. Complex **3**, which was prepared through a routine method using a salen-type ligand **1** bearing small methyl substituents and four quaternary ammonium salt units (eq 1), shows a turnover frequency (TOF) exceeding 10 000 h^{-1} and produces a strictly alternating copolymer with a high molecular weight (M_n) of up to

*To whom correspondence should be addressed. E-mail: bunyeoul@ajou.ac.kr.

(1) (a) Luinstra, G. A. *Polym. Rev.* **2008**, *48*, 192. (b) Darensbourg, D. J. *Chem. Rev.* **2007**, *107*, 2388. (c) Coates, G. W.; Moore, D. R. *Angew. Chem., Int. Ed.* **2004**, *43*, 6618. (d) Inoue, S.; Koinuma, H.; Tsuruta, T. *J. Polym. Sci. Part B: Polym. Lett* **1969**, *7*, 287. (e) Inoue, S.; Koinuma, H.; Tsuruta, T. *Makromol. Chem.* **1969**, *130*, 210.

(2) S, S.; Min, J. K.; Seong, J. E.; Na, S. J.; Lee, B. Y. *Angew. Chem., Int. Ed.* **2008**, *47*, 7306.

(3) (a) Kember, M. R.; Knight, P. D.; Reung, P. T. R.; Williams, C. K. *Angew. Chem., Int. Ed.* **2009**, *48*, 931. (b) Noh, E. K.; Na, S. J.; S, S.; Kim, S.-W.; Lee, B. Y. *J. Am. Chem. Soc.* **2007**, *129*, 8082. (c) Lee, B. Y.; Kwon, H. Y.; Lee, S. Y.; Na, S. J.; Han, S.-i.; Yun, H.; Lee, H.; Park, Y.-W. *J. Am. Chem. Soc.* **2005**, *127*, 3031. (d) Bok, T.; Yun, H.; Lee, B. Y. *Inorg. Chem.* **2006**, *45*, 4228. (e) Xiao, Y.; Wang, Z.; Ding, K. *Chem.—Eur. J.* **2005**, *11*, 3668. (f) Piesik, D. F.-J.; Range, S.; Harder, S. *Organometallics* **2008**, *27*, 6178. (g) Cui, D.; Nishiura, M.; Tardif, O.; Hou, Z. *Organometallics* **2008**, *27*, 2428.

(4) (a) Cohen, C. T.; Chu, T.; Coates, G. W. *J. Am. Chem. Soc.* **2005**, *127*, 10869. (b) Qin, Z.; Thomas, C. M.; Lee, S.; Coates, G. W. *Angew. Chem., Int. Ed.* **2003**, *42*, 5484. (c) Paddock, R. L.; Nguyen, S. T. *Macromolecules* **2005**, *38*, 6251. (d) Sugimoto, H.; Kuroda, K. *Macromolecules* **2008**, *41*, 312.

(5) (a) Darensbourg, D. J.; Phelps, A. L.; Gall, N. L.; Jia, L. *Acc. Chem. Res.* **2004**, *37*, 836. (b) Darensbourg, D. J.; Moncada, A. I. *Inorg. Chem.* **2008**, *47*, 10000. (c) Darensbourg, D. J.; Mackiewicz, R. M. *J. Am. Chem. Soc.* **2005**, *127*, 14026. (d) Darensbourg, D. J.; Bottarelli, P.; Andreatta, J. R. *Macromolecules* **2007**, *40*, 7727.

Published on Web 09/25/2009

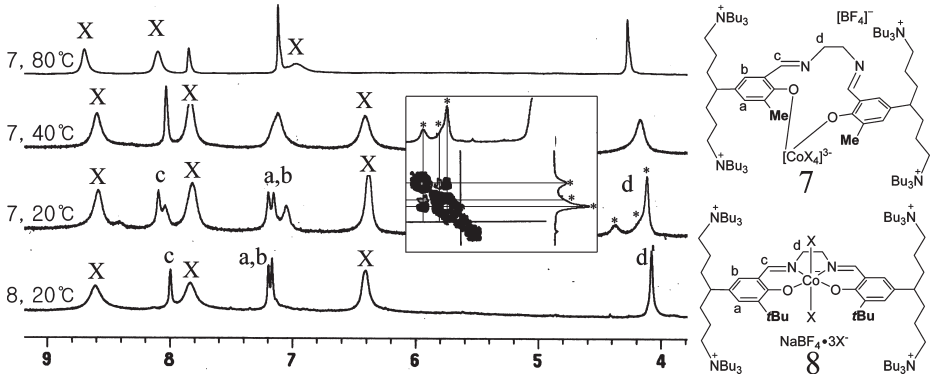

Figure 1. The ^{1}H NMR spectra of **7** and **8** in DMSO-d_6. The signals marked with "X" are assigned to 2,4-dinitrophenolate. The box shows a selected region of the ^{1}H−^{1}H COSY NMR spectrum of **7** at 20 °C.

300 000 and a high selectivity (> 99%). Another advantage of **3** is that the catalyst can be efficiently removed after polymerization from a polymer solution through filtration over a short pad of silica gel. The collected catalyst on the silica surface can then be recovered and reused. Removing the catalyst residue is crucial for copolymerization not only because catalyst residue colors the resin but also because it causes toxicity as well as severe depolymerization during thermal processing and storage.[6]

The structure of **3** was identified as that of a conventional tetradentate salen−cobalt(III) complex. The ^{1}H and ^{13}C NMR signals in DMSO-d_6 at room temperature are very complex. However, they are simplified to a set of broad signals at 40 °C and become sharper after raising the temperature to 80 °C, thereby allowing assignment to a conventional salen−cobalt(III) complex. Complex **4** is prepared from ligand **2**, in which the methyl substituent in **1** is replaced with *tert*-butyl. Unexpectedly, **4** exhibits a low activity ∼1/20 of that of **3** (TOF, 1 300 h^{-1}) along with a lower selectivity (84%). This difference in performance is contradictory to other reports. It was previously reported that a bulky *tert*-butyl group is required to attain high activity in the case of the binary system [salen−Co(III) complex]/[quaternary ammonium salt].[7] salen−cobalt complexes have been applied as versatile catalysts in various asymmetric syntheses, such as the hydrolytic kinetic resolution (HKR),[8] the nitro−aldol reaction,[9] the alkene hydrocyanation,[10] and the resolution of racemic *N*-benzyl α-amino acids.[11] In all these reactions, the utilized complexes were constructed from salicylaldehyde having a *tert*-butyl substituent on its 3-position. Complexes containing a methyl substituent instead of *a tert*-butyl have rarely been reported.[11] The large disparity in activity difference between **3** and **4** as well as the complicated and broad NMR signals of **3** promoted us to investigate thoroughly the structure of the highly active catalyst **3**. We reveal in this work that **3** adopts an unusual uncoordinated imine binding mode.

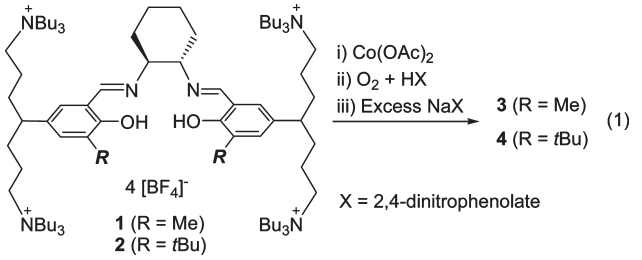

(1)

Results

NMR Studies. We prepared ethylenediamine-derived analogues using the same method and conditions as were used for the preparation of **3** and **4**, starting from the corresponding salen ligands **5** and **6** (eq 2). Since ^{15}N nuclei-labeled ethylenediamine is commercially available, ^{15}N NMR studies as well as ^{1}H and ^{13}C NMR studies could be performed. The ^{1}H, ^{13}C, and ^{15}N NMR spectra of **7** and **8** in DMSO-d_6 are significantly different from each other (Figures 1−3). For **8**, which bears a *tert*-butyl substituent, the ^{1}H NMR signals are normal; a set of sharp aromatic signals that belong to a salen unit is observed along with broad 2,4-dinitrophenolate (DNP) signals. The integration ratio of the number of DNP per salen unit is also as expected, ∼5.0. The ^{13}C NMR spectrum at 25 °C is also normal and belongs to the structure of a conventional tetradentate salen−cobalt(III) complex. The ^{15}N NMR signal at 25 °C is observed at −163.43 ppm as a sharp singlet.

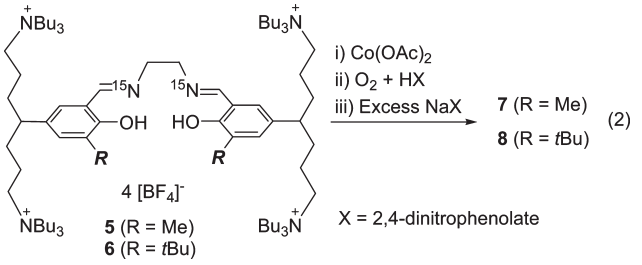

(2)

On the contrary, the ^{1}H NMR signal pattern (DMSO-d_6) of **7** at room temperature is abnormal, broad, and very

(6) Hongfa, C.; Tian, J.; Andreatta, J.; Darensbourg, D. J.; Bergbreiter, D. E. *Chem. Commun.* **2008**, 975.

(7) (a) Lu, X.-B.; Shi, L.; Wang, Y.-M.; Zhang, R.; Zhang, Y.-J.; Peng, X.-J.; Zhang, Z.-C.; Li, B. *J. Am. Chem. Soc.* **2006**, *128*, 1664. (b) Cohen, C. T.; Thomas, C. M.; Peretti, K. L.; Lobkovsky, E. B.; Coates, G. W. *Dalton Trans.* **2006**, 237.

(8) (a) Zheng, X.; Jones, C. W.; Weck, M. *J. Am. Chem. Soc.* **2007**, *129*, 1105. (b) Kunaga, M. T.; Larrow, J. F.; Kakiuchi, F.; Jacobsen, E. N. *Science* **1997**, *277*, 936. (c) Schaus, S. E.; Brandes, B. D.; Larrow, J. F.; Tokunaga, M.; Hansen, K. B.; Gould, A. E.; Furrow, M. E.; Jacobsen, E. N. *J. Am. Chem. Soc.* **2002**, *124*, 1307.

(9) Park, J.; Lang, K.; Abboud, K. A.; Hong, S. *J. Am. Chem. Soc.* **2008**, *130*, 16484.

(10) (a) Gaspar, B.; Carreira, E. M. *Angew. Chem., Int. Ed.* **2007**, *46*, 4519. (b) Gaspar, B.; Carreira, E. M. *Angew. Chem., Int. Ed.* **2008**, *47*, 5758.

(11) Dzygiel, P.; Reeve, T. B.; Piarulli, U.; Krupicka, M.; Tvaroska, I.; Gennari, C. *Eur. J. Org. Chem.* **2008**, 1253.

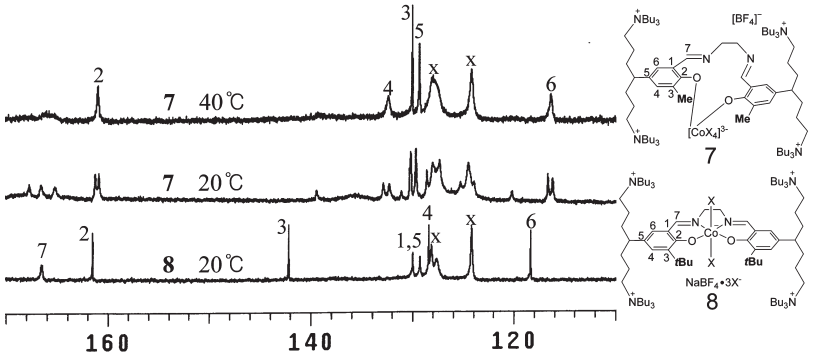

Figure 2. The ^{13}C NMR spectra of **7** and **8** in DMSO-d_6.

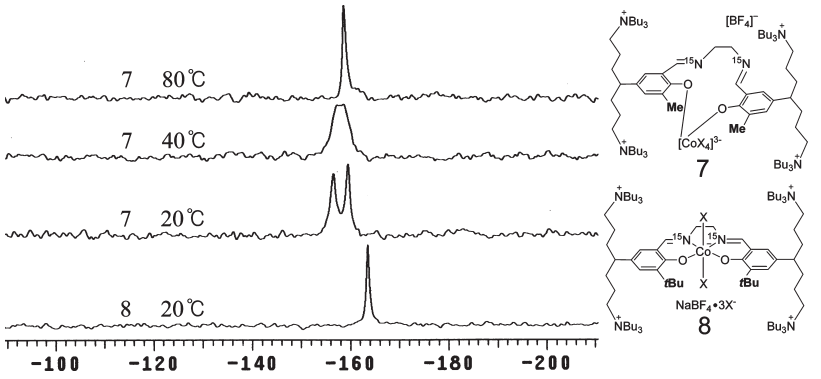

Figure 3. The ^{15}N NMR spectra of **7** and **8** in DMSO-d_6.

complicated, which differs significantly from that of **8**. Raising the temperature to 40 °C collapses some signals into a fairly assignable spectrum, despite some remaining quite broad. Raising the temperature to 80 °C even further develops a set of sharp signals. The integration ratio of the number of DNP per salen unit is not close to ~5.0 but is to ~4.0. The ^{13}C NMR spectrum at 25 °C is also too complicated to be simply assigned a conventional tetradentate salen−cobalt(III) structure. At 40 °C, the pattern becomes simplified, but still some very broad signals are present. The ^{15}N NMR spectrum is also strikingly different from that of **8**. Two moderately sharp signals are observed at −156.32 and −159.21 ppm, which are shifted downfield from the chemical shift of the *tert*-butyl complex (−163.43 ppm) at room temperature. Raising the temperature to 40 °C collapses the two signals into a broad single signal, which then becomes sharp after the temperature is raised to 80 °C.

The ^1H NMR spectra of **7** and **8** in THF-d_8 or CD_2Cl_2 also have very different patterns (Figure 4). For the ^1H NMR spectrum of **8** in THF-d_8, a set of salen signals is observed along with very broad DNP signals. Some very broad signals are observed at an abnormal region (−2−0 ppm) due to the presence of a paramagnetic species. For the ^1H NMR spectrum of **7** in THF-d_8, a set of salen signals is observed, but the chemical shifts of the aromatic salen protons (6.90, 7.05, and 7.93 ppm) and that of the NCH_2CH_2N unit (4.51 ppm) are fairly different from those observed for the *tert*-butyl complex **8** (7.12, 7.31, 7.74, and 4.18 ppm, respectively). Interestingly, the DNP signals are broad at 7.88, 8.01, and 8.59 ppm, and the integration ratio of number of DNP per salen unit is ~2.0. The ^1H NMR spectra of **7** and **8** in CD_2Cl_2 have features that are almost identical with those observed in THF-d_8 (Figure 4).

In the ^{15}N NMR spectrum of **8** in THF-d_8, a sharp singlet signal is observed at −166.80 ppm. A sharp singlet signal is also observed but significantly shifted downfield at −154.32 ppm in the ^{15}N NMR spectrum of **7**. This difference in chemical shift (Δppm = 12.5) is too big to be explained with only a substituent effect. It was reported that the ^{15}N NMR chemical shifts of imine ($-N{=}C-C_4H_4-X$) and hydrazone ($N-N{=}C-C_4H_4-X$) fit well to the Hammett-type equation with a slope of ρ = ~10.[12] Considering the σ values of methyl and *tert*-butyl substituents (σ_m = −0.06, σ_p = −0.14, and σ^+ = −0.31 for methyl; σ_m = −0.09, σ_p = −0.15, and σ^+ = −0.26 for *tert*-butyl), the estimated chemical shift difference (Δppm) should not be so large. In fact, the chemical shift difference observed in the ligand stage is only 2.86 ppm (−63.68 ppm for **5**; −66.54 ppm for **6**). The reported substituent effect on the ^{15}N NMR chemical shifts is also not as large for dipyrrolmethenes and their Zn(II) complexes, as evidenced by only 2.0 ppm difference when hydrogen was replaced with ethyl in the pyrrol ring of the Zn(II) complex.[13] Therefore, the large chemical shift difference observed in the ^{15}N NMR studies (Δppm = 12.5), along with the significant differences between the ^1H and ^{13}C NMR spectra, leads us to propose that **7** adopts a binding mode that differs from the typical tetradentate salen−Co(III) structure of **8**. The ^{15}N NMR signal of **7** in THF-d_8 becomes significantly broadened after the temperature is lowered to −75 °C (full width at half-maximum (fwhm), ~10 ppm), while that of **8** is persistently

(12) Neuvonen, K.; Fülöp, F.; Neuvonen, H.; Koch, A.; Kleinpeter, E.; Pihlaja, K. *J. Org. Chem.* **2003**, *68*, 2151.
(13) Wood, T. E.; Berno, B.; Beshara, C. S.; Thompson, A. *J. Org. Chem.* **2006**, *71*, 2964.

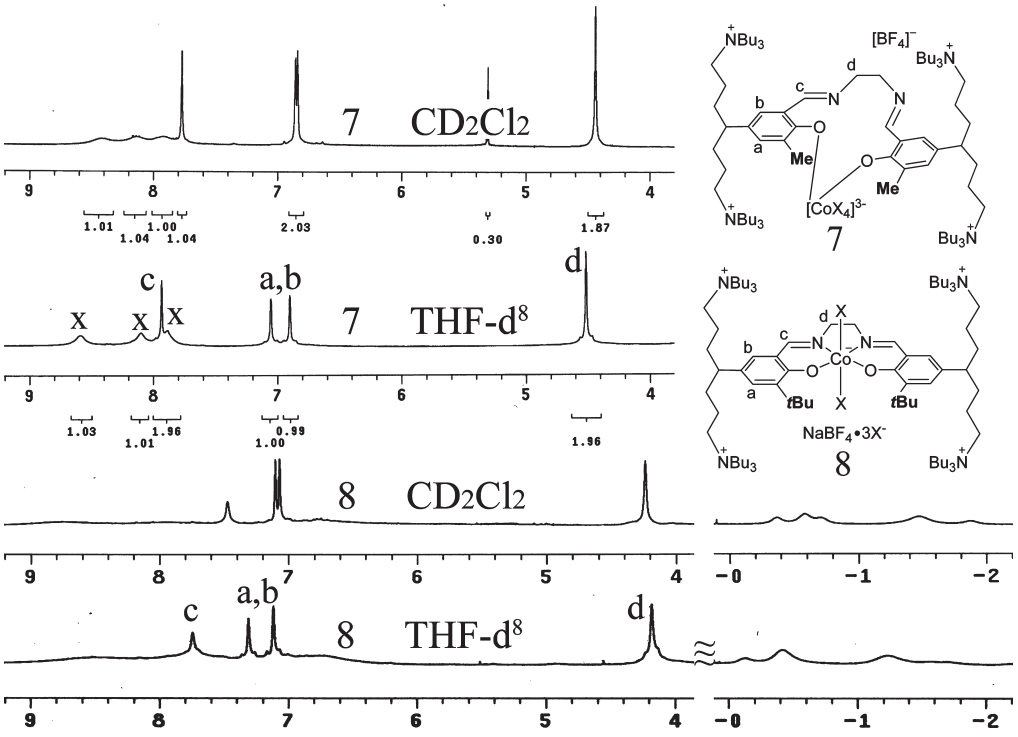

Figure 4. The ^{1}H NMR spectra of **7** and **8** in THF-d_8 and CD_2Cl_2.

sharp (fwhm, ~1.5 ppm at −75 °C). These variable temperature ^{15}N NMR studies suggest that **7** adopts some flexible structure.

The IR spectra of **7** and **8** are also significantly different from each other, especially in the $-NO_2$ symmetric vibration region that is located between 1 200 and 1 400 cm^{-1} (Figure 5). In the spectrum of the methyl complex **7**, a very broad band at the region seems to be an overlap of several sets of signals. In the spectrum of the *tert*-butyl complex **8**, there are signals that are similar to those of sodium 2,4-dinitrophenolate, but are slightly shifted to a lower frequency (main signal from 1 350 to 1 315 cm^{-1}).

Proposal for Uncoordinated Imine Structure. The ^{1}H, ^{13}C, and ^{15}N NMR spectra of the *tert*-butyl complex **8** can be assigned to a structure of the conventional tetradentate salen−cobalt(III) complex (Chart 1). One equivalent of $NaBF_4$ is incorporated during the salt exchange reaction, which is supported by the observation of typical BF_4 signals (two broad signals at −50.65 and −50.70 ppm) in the ^{19}F NMR spectrum and by the detection of an equivalent amount of Na^+ ions in the ICP-AES. DNP proton signals in DMSO-d_6 are broad and even broader in THF-d_6 and CD_2Cl_2, indicating DNP ligands are fluxional between a coordinated and an uncoordinated state. A paramagnetic, five-coordinating, square-pyramidal structure is a mediator in this fluxional motion, thereby causing the incidence of abnormal signals at −2−0 ppm.[14]

We propose that **7** adopts an unusual uncoordinated imine structure (**7-A** in Chart 1) as opposed to a conventional one, **7-B**. DNP anions, which counter the quaternary ammonium cations, coordinate to cobalt instead of imine donors. We performed the anion exchange reaction of BF_4^- with DNPs by stirring the BF_4^- complex overnight in slurry of 5 equivalents (per cobalt) of NaDNP in CH_2Cl_2. The integration ratio of the number of DNP per salen unit is ~4.0, which is persistent even under conditions of more excess NaDNP (10 equivalents) and longer reaction times (2 days). That is, one of the four BF_4^- remains present and unexchanged with DNP. We also observe a typical BF_4 signal in the ^{19}F NMR spectrum of **7**. The ICP-AES study of **7** indicates a negligible amount of Na^+ ion contained in **7**.

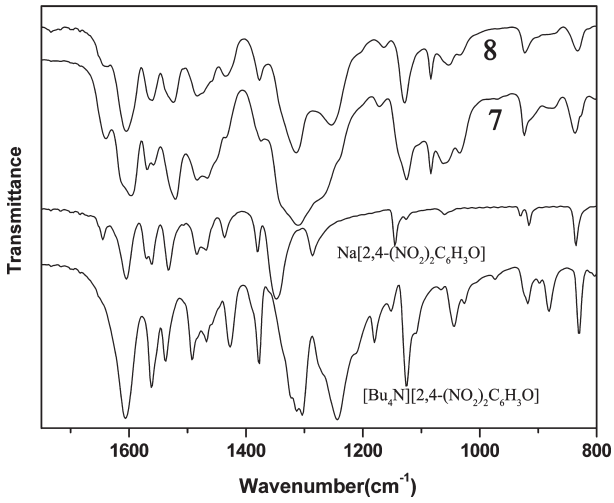

Figure 5. The IR spectra of **7**, **8**, sodium 2,4-dinitrophenolate, and tetrabutylammonium 2,4-dinitrophenolate.

Complex **9** is obtained from a similar salen-type ligand containing six quaternary ammonium salt units (Chart 1). In complex **9**, only three of the six BF_4 anions are

(14) (a) Konig, E.; Kremer, S.; Schnakig, R.; Kanellakopulos, B. *Chem. Phys.* **1978**, *34*, 379. (b) Kemper, S.; Hrobàrik, P.; Kaupp, M.; Schlörer, N. E. *J. Am. Chem. Soc.* **2009**, *131*, 4172.

Chart 1. Structures of salen−Co(III) complexes by variation of ligand structures (X = 2,4-dinitrophenolate)

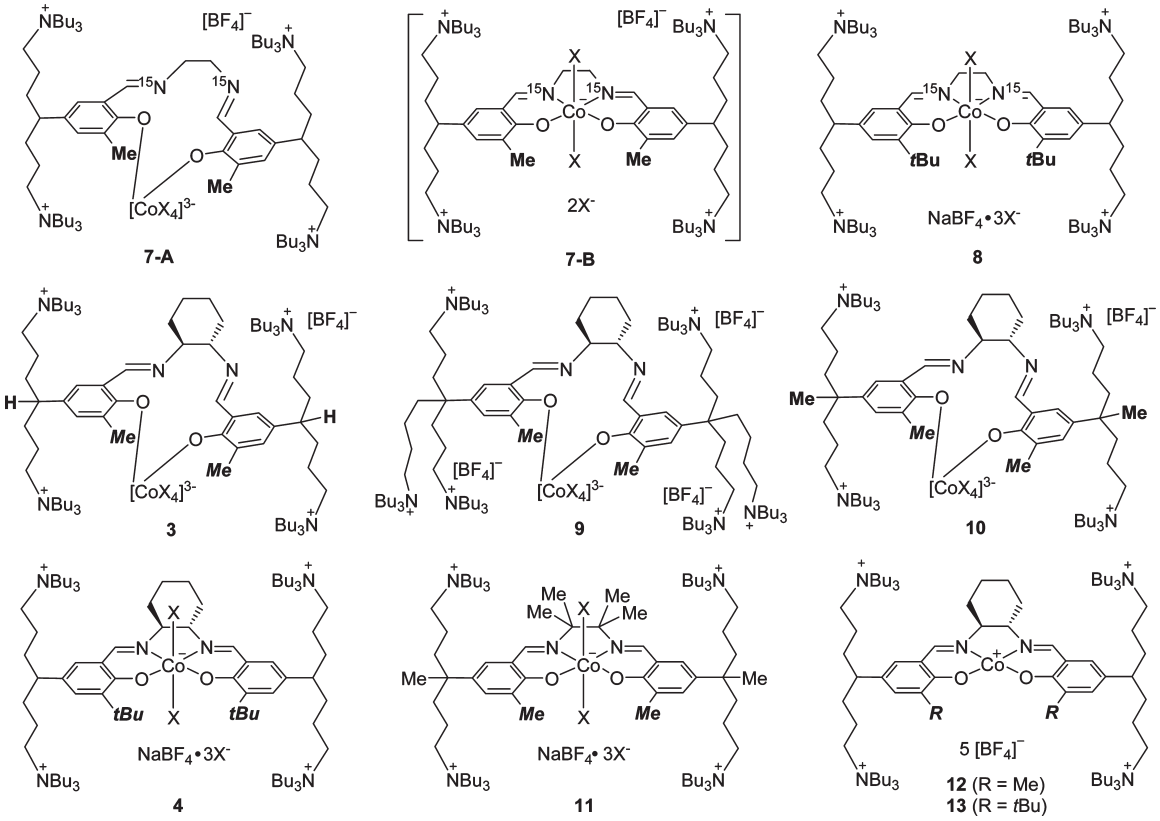

exchanged with DNPs, even though salt exchange is performed using 10 equivalents of NaDNP. Formation of an octahedral complex with a formal −3 charge on cobalt, coordinated by four DNPs and two salen−phenoxys, may drive the anion exchange reaction. The cobalt(III) ion is classified as a hard acid, preferring to be coordinating with hard oxygen donors such as DNPs as opposed to soft imine bases. For **8**, the bulky *tert*-butyl group blocks formation of such an octahedral structure, yielding a conventional imine-coordinating complex. Octahedral cobaltate(III) complexes with a formal −3 charge on cobalt are not rare.[15]

NMR signal behaviors of the highly active catalyst **3**, which was previously assigned a conventional imine-coordinating structure, are almost identical to those of **7** (Supporting Information). Therefore, we here reassign **3** as having an uncoordinated imine structure. Recently, we developed an efficient synthetic route for **10** in which the $-CH(CH_2CH_2CH_2N^+Bu_3)_2$ units in **3** are replaced with $-CMe(CH_2CH_2CH_2N^+Bu_3)_2$.[16] Complex **10** is easily prepared in 10s-gram scale compared to that of the relatively difficult preparation of **3**. The NMR signal behaviors of **10** and hexaammonium complex **9** are similar to those of **7**.

The NMR signal behaviors of **4**, which exhibits a significantly lower activity than **3**, are almost identical to those of **8**, which exhibits a conventional imine-coordinating structure. Complex **11** is prepared from a salen-type ligand constructed from $H_2N-CMe_2CMe_2-NH_2$ and salicylaldehyde containing a methyl substituent on its 3-position.[17] Interestingly, **11** shows the same features in its ^1H NMR spectrum as does **8**: a sharp aromatic signal as well as a paramagnetic signal at −2−0 ppm in DMSO-d_6. Therefore, complex **11** should be assigned a conventional imine-coordinating structure.

DFT Calculations. We performed DFT calculations to compare the energy level of the proposed uncoordinated imine structure **7-A** to that of its isomeric form **7-B**, a conventional imine-coordinating structure. In structure **7-A**, two salen−phenoxys are fixed to be coordinating in cis configuration with cobalt along with four DNPs at other sites of the octahedron. In structure **7-B**, the conventional salen−Co(III) architecture forms an octahedron with two DNPs on the axial sites. Two additional DNP anions as well as a BF_4^- are around in the outer sphere as counter anions. The tributylammonium units are abbreviated as trimethylammonium units in order to reduce the calculation time. According to computational calculations, the structure **7-A** is more stable than the structure **7-B** by ca. 34 kcal/mol. This amount of energy difference is substantial; the structure of the complex prepared from the methyl ligand **5** by eq 2 can, thus, be reasonably assigned to **7-A**. Figure 6 shows the energy-minimized conformations of the structure **7-A** and **-B** obtained by the DFT calculations.

Status of DNP Ligands. In methylene chloride, the medium of the final anion exchange reaction, broad

(15) (a) Yagi, T.; Hanai, H.; Komorita, T.; Suzuki, T.; Kaizaki, S. *J. Chem. Soc., Dalton Trans.* **2002**, 1126. (b) Fujita, M.; Gillards, R. D. *Polyhedron* **1988**, *7*, 2731.

(16) Min, J.; Seong, J. E.; Na, S. J.; Cyriac, A.; Lee, B. Y. *Bull. Korean Chem. Soc.* **2009**, *30*, 745.

(17) Boettcher, A.; Elias, H.; Jaeger, E. G.; Langfelderova, H.; Mazur, M.; Mueller, L.; Paulus, H.; Pelikan, P.; Rudolph, M.; Valko, M. *Inorg. Chem.* **1993**, *32*, 4131.

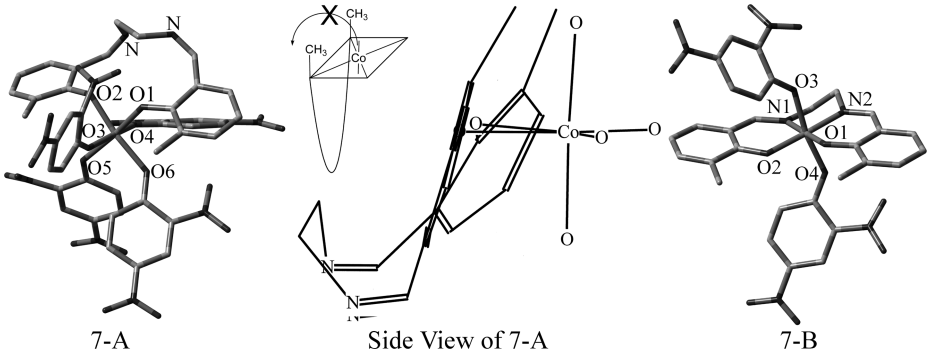

Figure 6. The most stable conformation of the structures of **7-A** and **-B** calculated by DFT calculations ($-CH(CH_2CH_2CH_2N^+Bu_3)_2$ units are deleted for simplification).

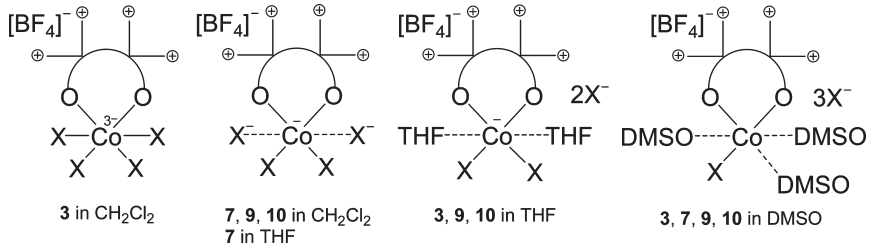

Figure 7. Cartoons showing the status of DNP ligands at room temperature when solvent and ligand structure are varied (X = 2,4-dinitrophenolate).

DNP signals are observed at 8.4, 8.1, and 7.9 ppm in the ^{1}H NMR spectra of **7**, **9**, and **10**, which adopt an uncoordinated imine structure. The integration ratio of number of DNP per salen unit is ~2.0, which is half of that observed in DMSO-d_6 (Figure 4). This means that only two of the four DNPs are detected in the ^{1}H NMR spectra, whereas the other two are missing possibly due to severe broadening. For complex **3**, all four DNP signals are observed at the same region. Since the chemical shifts of the observed DNP signals are significantly different from those of $[Bu_4N]^+[DNP]^-$ (8.77, 7.85, and 6.48 ppm), they can be assigned to coordinating DNPs. These NMR data indicate that all four DNPs of **3** stay in a persistently coordinated state in CH_2Cl_2. However, for **7**, **9**, and **10**, two of the four DNPs persistently stay in a coordinated state, while the other two are fluxional between a coordinated and an uncoordinated state. Fluxional movement occurs in NMR time scales and with almost unbiased probability, making average signals unobservably broad. Figure 7 shows cartoons describing the status of DNP ligands when the solvent and the ligand structures are varied.

At room temperature, the ^{1}H NMR spectrum of **7** in THF-d_8 contains only two coordinating DNPs, which are detected as broad signals at 8.6, 8.1, and 7.9 ppm (Figure 8). The other two DNPs are missing due to signal broadening. When the temperature is lowered to 0 °C, the DNP signals become sharpened and display a coupling pattern. By correlating the coupling pattern and the analysis of the ^{1}H−^{1}H COSY spectrum (Supporting Information), the coordinating DNP signals are able to be unambiguously assigned (Figure 8). When the temperature is lowered further to −25 °C, a new set of broad DNP signals, which are marked as "*" in Figure 8, is observed at 8.8 ppm as a shoulder of the coordinating DNP signal, at 7.9 ppm collapsed with the coordinating DNP signal, and at 6.5 ppm isolated from other signals. Since these chemical shifts are close to those of $[Bu_4N]^+DNP^-$ (8.68, 7.78, and 6.38 ppm in THF-d_8), we assign them to a mostly uncoordinated, fluxional DNP signal. When the temperature is raised to 70 °C, all four DNP signals become severely broadened as a single set of signals at 9.3, 9.0, and 7.8 ppm. Figure 8 shows the variable temperature ^{1}H NMR spectra with cartoons that describe the status of DNPs at each temperature. As the temperature increases, DNPs more tightly interact with the cobalt center. Since uncoordinated DNPs are prone to being solvated, the decoordinating process is, therefore, entropy sacrificing and more favorable at low temperatures. Lowering the temperature causes a similar equilibrium shift from contact ion pairs toward solvent separated ion pairs in other systems.[18]

Variation of the DNP signal pattern in the variable temperature ^{1}H NMR studies of **8** in thf-d_8 is different from that observed for **7** (Supporting Information). Lowering the temperature to 0 °C severely broadens the DNP signals such that almost all become missing. At −25 °C, a set of relatively sharp DNP signals is observed at 8.1, 7.6, and 6.8 ppm with an integration ratio of the number of DNP per salen unit being ~2.0. Another set of very broad DNP signals are present at 8.9, 8.0, and 6.8 ppm whose chemical shifts are close to those of uncoordinated DNP in **7** (8.7, 8.0, and 6.8 ppm). At −50 °C, the very broad signals are sharpened and revealed clearly two sets of DNP signals. We assign one set of these (8.1, 7.6, and 6.8 ppm) to DNPs coordinating at the axial sites of a conventional tetradentate salen-structure, whereas the other set (8.9, 8.0, and 6.8 ppm) is assigned to an uncoordinated one.

(18) (a) Streitwieser, A., Jr.; Chang, C. J.; Hollyhead, W. B.; Murdoch, J. R. *J. Am. Chem. Soc.* **1972**, *94*, 5288. (b) Hogen-Esch, T. E.; Smid, J. *J. Am. Chem. Soc.* **1966**, *88*, 307. (c) Lü, J.-M.; Rosokha, S. V.; Lindeman, S. V.; Neretin, I. S.; Kochi, J. K. *J. Am. Chem. Soc.* **2005**, *127*, 1797.

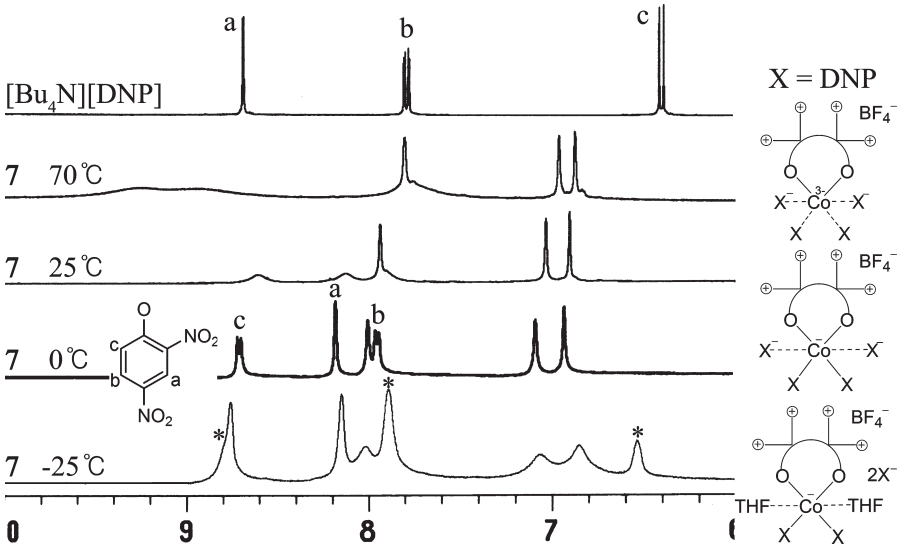

Figure 8. Variable temperature ^{1}H NMR spectra of **7** in THF-d_8.

The status of the DNPs in THF varies depending upon ligand structure. In the ^{1}H NMR spectrum of **7**, a set of coordinating DNP signals is observed with an integration value of ~2 for the number of DNP per salen unit. The other two DNPs are missing, indicating they are fluxional between a coordinated and an uncoordinated state with almost unbiased probabilities. On the contrary, all the four DNPs are observed in **3**, **9** and **10**. Specifically, two sets of DNP signals are clearly present at an almost 1:1 ratio in the ^{1}H NMR spectrum of **3** at room temperature. One set (8.7, 8.2, and 7.8 ppm) is assigned to the coordinating DNPs, while the other set (8.8, 7.8, and 6.4 ppm) is assigned to fluxional, mostly uncoordinated DNPs. In the ^{1}H NMR spectra of **9** and **10**, two sets of DNP signals are also observed. However, the fluxional DNP signals are much broader, indicating those in **9** and **10** stay a little more in a coordinated state than those in **5**. Therefore, the order of binding affinity of the two fluxional DNPs is **7** > **9** and **10** > **3**.

At 40 °C in DMSO-d_6, the chemical shifts of DNP (8.6, 7.8, and 6.4 ppm) in the ^{1}H NMR spectra of **3**, **7**, **9**, and **10** are similar to those of $[Bu_4N]^+DNP^-$ (8.58, 7.80, and 6.35 ppm in DMSO-d_6). However, the signals of DNP are broad, while those of $[Bu_4N]^+DNP^-$ are very sharp. At room temperature, another set of DNP signals, which can be assignable to a coordinating DNP, is observed at 8.5, 8.1, and 7.8 ppm with roughly one-third the intensity of the main uncoordinated DNP signals (Figure 1 and Supporting Information). Therefore, as shown in Figure 7, one DNP stays in a coordinated state, while the other three DNPs stay mostly in uncoordinated state when in DMSO at room temperature.

Analysis of the NMR Spectra in DMSO-d_6. The ^{1}H, ^{13}C, and ^{15}N NMR spectra of **7** in DMSO-d_6 at room temperature are very complicated but explainable by the proposed structure of **7-A** as well as the status of DNPs. In Figure 7, the octahedral cobalt is coordinated by three DMSOs, one DNP, and two salen−phenoxys. In this situation, the two phenoxys in a salen unit are inequivalent; one is situated in trans with DMSO, while the other is in trans with DNP. Hence, we observe two signals in the ^{15}N NMR spectrum at room temperature (Figure 3) along with the splitting of aromatic signals in the ^{1}H and ^{13}C NMR spectra (Figures 1 and 2). The signals for NCH_2CH_2N in the ^{1}H NMR spectrum are observed split at 4.3, 4.15, and 4.1 ppm in a 1:1:2 ratio. The ^{1}H−^{1}H COSY NMR spectrum proves that the three signals arise from a NCH_2CH_2N unit, not from a mixture of three different conformations or configurations (Figure 1). In the energy-minimized conformation of **7-A**, flip of the cobalt octahedron from a side of the macrocycle to the other side is not allowed (Figure 6) under which condition the cobalt square plane formed by a DMSO, a DNP, and two salen−phenoxys has a planar chirality. Similar planar chirality in cyclophane-type imidazole was recently reported.[19] Upon generation of a chiral center, two protons attached to a $N-CH_2$ unit become diastereotopic to each other, making it possible for them to be observed separately. For complexes such as **3** and **10**, which contain chiral centers in their salen-type ligand, planar chirality in the cobalt octahedron results in generation of two diastereomers, which make the ^{1}H and ^{13}C NMR signals more complicated (see Supporting Information).

Raising the temperature to 40 °C collapses the coordinating DNP signals into a set of very broad signals. In this situation, the asymmetrical coordination environment is broken, and hence, a set of simplified salen-ligand signals is observed. In THF and CH_2Cl_2, the coordination environment surrounding cobalt is symmetrical even at room temperature (Figure 7), and hence, a set of sharp salen signals is observed in the ^{1}H, ^{13}C, and ^{15}N NMR spectra.

Cyclic Voltammetric Studies. Cyclic voltammetric (CV) studies also suggest that **3** and **4** adopt different binding modes. If **3** and **4** had the same binding mode, then a more facile reduction of methyl complex **3** would be expected because methyl is less electron-donating than *tert*-butyl. The opposite result is observed in the CV studies: reduction of *tert*-butyl complex **4** is easier than that of methyl complex **3**. The $E_{1/2}$ values for Co(III/II) are −0.076 and

(19) Ishida, Y.; Iwasa, E.; Matsuoka, Y.; Miyauchi, H.; Saigo, K. *Chem. Commun.* **2009**, 3401.

−0.013 V versus SCE for **3** and **4**, respectively. The observed potential difference ($\Delta E_{1/2}$ for Co(III/II)) of 63 mV is not trivial considering that a potential difference of 59 mV means the ratio of [Co(II)] to [Co(III)] differs by 10-fold at the same electrochemical potential, which is inferred from the Nernst equation ($E = E^{o} + (0.0592) \log\{[ox]/[red]\}$).

Complexes **12** and **13** (chart 1) contain five BF_4 anions but no DNP anions. We can expect the same binding mode of a conventional imine-coordinating structure, especially in a noncoordinating solvent such as CH_2Cl_2. CV studies in CH_2Cl_2 find the same $E_{1/2}$ value for Co(III/II) for both complexes at 0.63 V versus SCE. This result implies that changing the methyl substituent with *tert*-butyl has a negligible influence on the $E_{1/2}$ value for Co(III/II) once the complexes adopt the same binding mode. By changing the solvent from CH_2Cl_2 to DMSO, the $E_{1/2}$ values for Co(III/II) of **12** and **13** become differentiated at −0.074 and −0.011 V versus SCE, respectively. These values are almost identical with those observed for **3** and **4** in DMSO (−0.076 and −0.013 V versus SCE, respectively). DMSO is a good ligand especially for a hard Co(III) center. Therefore, a conventional imine-coordinating binding mode switches to an uncoordinated imine binding mode in DMSO, where cobalt is coordinated by four DMSOs and two salen−phenoxys. A single sharp signal is observed at −159.11 ppm (DMSO-d_6) in the ^{15}N NMR spectrum of the complex containing five BF_4 anions, which is prepared from a ^{15}N-labeled ligand **5**. This observed chemical shift is close to that of **7** (−158.35 ppm at 40 °C) but not to that of **8** (−163.43 ppm), which is evidence of four coordinated DMSOs and an uncoordinated imine binding mode in DMSO.

Initiation Reaction. Nothing is changed in the ^1H NMR spectrum of **10** when CO_2 gas is added to the THF-d_6 solution. This implies that DNPs in **10** do not attack CO_2. However, **10** reacts with PO, increasing new signals that are marked with "*" in Figure 9. These new signals are assigned to an anion illustrated in structure **14** (eq 2). Attack of PO by the DNP anion generates an alkoxide anion, which then intramolecularly attacks the *ipso*-carbon. A salt containing this type of anion has been previously reported and termed the spiro-Meisenheimer complex.[20] Due to the stereochemistry of the methyl group, a diastereomerism is created that produces two sets of signals. The salen-aromatic signals observed at 7.0−7.4 ppm are very complicated but not due to destruction of the salen unit. Upon addition of acetic acid, the salen aromatic signals become a simple set of broad signals, whereas and the spiro-Meisenheimer anion becomes protonated to form a mixture of 2,4-$(NO_2)_2C_6H_3$−$OCH_2CH(Me)OH$ and 2,4-$(NO_2)_2C_6H_3$−$OCH(Me)CH_2OH$ (eq 3). Conversion of DNPs into the spiro-Meisenheimer anion is stopped when the integration values of DNP (6.3 ppm) and the spiro-Meisenheimer anion (6.8 ppm) signals are almost equal (∼1 h). Following this, the conversion rate is negligible, and the integration ratio of [spiro-Meisenheimer anion]/[DNP] is 1.1 at 2 h.

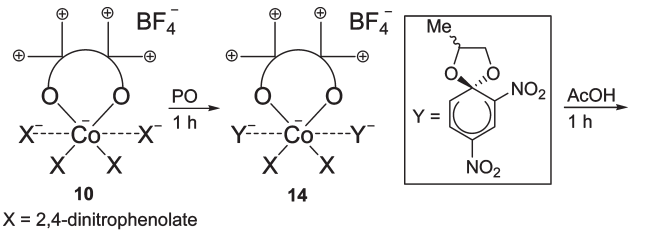

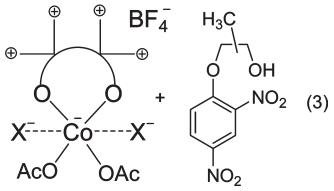

While the conversion rate is not altered by the addition of 5 equivalents of water per cobalt, it is significantly reduced by the addition of more water. In the presence of 25 and 50 equivalents of water, the integration ratio of [spiro-Meisenheimer anion]/[DNP] is reduced from 1.0 to 0.68 and 0.47, respectively, at 1 h. In the presence of 50 equivalent of water, the [spiro-Meisenheimer anion]/[DNP] ratios are only 0.53 and 0.63 at reaction times of 2 and 4 h, respectively, not reaching a 1.0 value (Figure 9).

The reaction pattern between PO and **8** is different from that between PO and uncoordinated imine complex **10**. The same spiro-Meisenheimer anion is generated, but its amount gradually increases and exceeds the stage of [spiro-Meisenheimer anion]/[DNP] = 1.0. The [spiro-Meisenheimer anion]/[DNP] ratio is 0.96 (1 h), 1.4 (2 h), 1.8 (7 h), and 2.0 (20 h). Another striking difference is that a significant amount of paramagnetic species (^1H NMR signals at −1 - 0.5 ppm) is formed, which amount gradually increases by the time.

CO_2/Propylene Oxide Copolymerization Studies. Complexes **6**, **8**, and **11** show poor catalytic performance (entries 2, 4, and 7 in Table 1), whereas complexes **3**, **7**, and **10** are excellent at polymerization conditions of [PO]/[Cat] = 1×10^5, temperature = 70−75 °C, and P_{CO_2} = 17−20 bar (entries 1, 3, and 6). Hexaammonium salt complex **9** does not produce any polymer at these conditions even though its coordination mode is identical to **3**, **7**, and **10** (entry 5). The order of activities (TOF) is **3** > **10** > **7**, which, interestingly, is opposite to the order observed for the binding affinity of the two loosely bound, fluxional DNPs with cobalt in THF.

Complex **10** is easily prepared in 10s-gram scale allowing feasibility in a commercial application.[16] In extensive polymerization studies with **10**, severe fluctuation of induction time (1−10 h) has been observed especially in hot and humid weather. After initiation, rather consistent TOFs are attained in the range of 9 000−11 000 h^{-1}. Typically, bimodal molecular weight distributions are observed for all copolymers obtained in this study, even though the M_w/M_n values are only in the range of 1.2−1.3 (Figure 10). The higher molecular weight portion is attributed to biaxial chain growth from water molecules, whereas the other lower portion is due to uniaxial chain

(20) (a) Fendler, E. J.; Fendler, J. H.; Byrne, W. E.; Griff, C. E. *J. Org. Chem.* **1968**, *33*, 4141. (b) Bernasconi, C. F.; Cross, H. S. *J. Org. Chem.* **1974**, *39*, 1054.

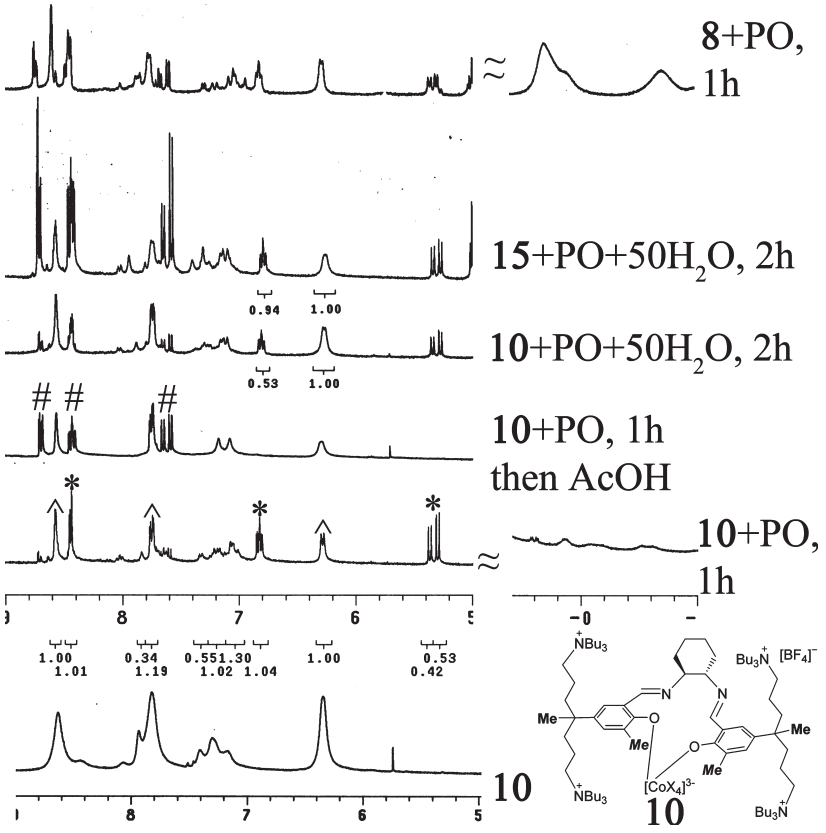

Figure 9. The ^{1}H NMR spectra (DMSO-d_6) showing the reaction between the complexes and the propylene oxide (* signals from spiro-Meisenheimer anion; ^ signals from DNP anion; # signals from protonated compound of the spiro-Meisenheimer anion).

Table 1. CO_2/PO Copolymerization Results[a]

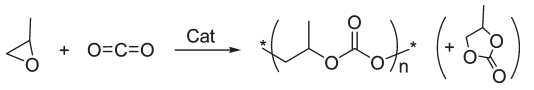

entry	cat	induction time (min)	TOF[b]	selectivity[c]	head-to-tail linkage (%)	M_n[d] ($\times 10^{-3}$)	M_w/M_n
1	**3**	60[e]	13 000	92	80	210	1.26
2	**4**[f]	0	1 300	84	85	38	2.34
3	**7**	120[e]	8 300	97	74	113	1.23
4	**8**	0	5 000	85	82	120	1.41
5	**9**		0				
6	**10**	260[e]	11 000	96	87	140	1.17
7	**11**		0				
8	**14**	30[g]	13 000	>99	87	170	1.21
9	**15**	0[g]	15 000	>99	84	270	1.26
10[h]	**15**	0	16 000	>99	82	300	1.31

[a] Polymerization condition: PO (10 g, 170 mmol), [PO]/[Cat] = 1×10^5, CO_2 (2.0−1.7 MPa), temperature = 70−75 °C, and reaction time = 60 min. [b] Calculated based on the weight of the isolated polymer including the cyclic carbonate. [c] Selectivity of the polycarbonate over the cyclic carbonate in unit of % as determined by ^{1}H NMR spectroscopy of the crude product. [d] Determined on GPC using the a polystyrene standard. [e] Induction times severely fluctuate batch to batch in the range of 1−10 h. [f] Polymerization data in [PO]/[Cat] = 2.5×10^3 from ref 2. [g] Induction times of < 1 h are observed in many other batches. [h] Large scale polymerization using 230 g of PO.

growth from DNPs.[21] An interesting trend is observed in the GPC traces: the longer the induction time, the lower the molecular weight (M_n) and the larger the portion of polymer chains that are grown from water (Figure 10 and Table 1). This feature indicates that the long induction time is related to water. Diffusion of water into a glovebox through gloves and a polycarbonate panel are substantial in a hot and humid climate.[22] Failure in maintaining water levels in the glovebox, in which the reactor is assembled, may be a cause of a fluctuating induction time.

A slow rate of initiation (DNP attack onto PO) in the presence of water is also found in the NMR studies (Figure 9). Complex **14** (Chart 2) is prepared by reacting

(21) Nakano, K.; Kamada, T.; Nozaki, K. *Angew. Chem., Int. Ed.* **2006**, *45*, 7274.

(22) Shriver, D. F.; , Drezdzon, M. A. *The Manipulation of Air-Sensitive Compounds* 2nd ed.; John Wiley & Sons: Singapore, 1986; pp 52−54.

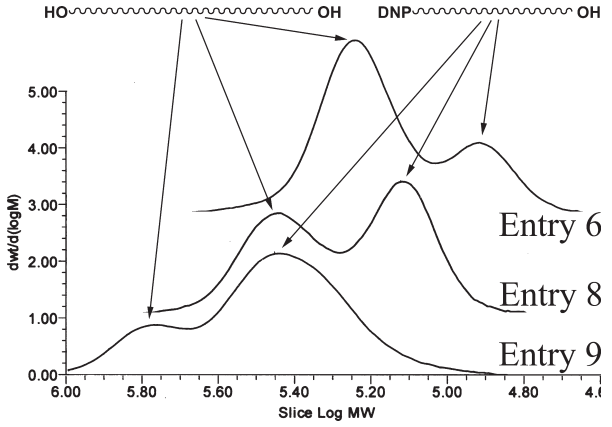

Figure 10. The GPC traces of polymers.

a high concentration of **10** with/in PO for 1 h such that the ratio of [residual water in PO]/[**10**] is negligible. Complex **14** is not as sensitive as **10** and is more consistent in its polymerization for induction times below 1 h (entry 8).

Dinitrophenol−Dinitrophenolate Homoconjuation as the Initiating Anion. Better and consistent catalytic performances are obtained when 60 mol % NaDNP containing 40 mol % 2,4-dinitrophenol (DNP-H) is employed at the final anion exchange reaction in Equation 1. A student mistakenly added commercial 60% NaH instead of oil-washed 100% NaH during the preparation of five equivalents of pure NaDNP from DNP-H.[23] Therefore, approximately three equivalents of NaDNP plus two equivalents of DNP-H were added to the anion exchange reaction. In the ^{1}H NMR spectrum of the complex prepared using the 60 mol % NaDNP, a set of broad DNP-related signals is observed in DMSO-d_6 with a [DNP + DNP-H]/[salen] signal ratio of ∼6. We presume that a complex, where two 2,4-dinitrophenolate−2,4-dinitrophenol homoconjugations ($[DNP\cdots H\cdots DNP]^-$) are loosely bound on cobalt, was created by the mistake (**15** in chart 2). It is well-established that a hydrogen bond between a proton donor and an acceptor whose $\Delta pK_a = 0$ is extraordinarily strong, especially in an aprotic solvent.[24] The distance between the oxygens in the solid structure of (18-crown-6-κ^6O) potassium 2,4-dinitrophenolate−2,4-dinitrophenol homoconjugation is very short (2.453(4) Å), supporting a very strong hydrogen bond.[25] The formation constant of homoconjugation for $[DNP\cdots H\cdots DNP]^-$ was determined electrochemically in acetonitrile to be ∼100.[26] In the ^{1}H NMR spectrum of **15** in THF-d_6, two sets of DNP signals are observed; one set is assigned to a coordinating DNP, while the other set, whose chemical shifts resemble a mixture of $[Bu_4N]^+[DNP]^-$ and 2,4-dinitrophenol (1:1) in THF-d_8, is assigned to the homoconjugation (Supporting Information).

Complex **15** is not so sensitive toward water as **10**, providing consistent polymerization performance with low induction times (< 1 h). Furthermore, it provides

Chart 2. Salen−Co(III) Complex Showing an Excellent Catalytic Performance (X = 2,4-Dinitrophenolate)

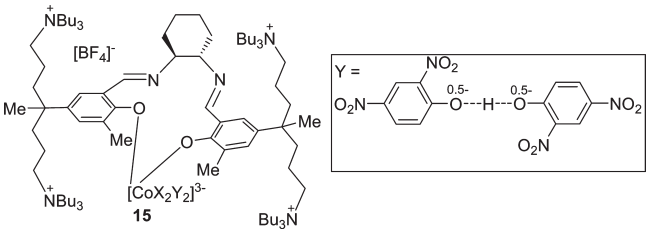

∼1.5 times higher TOFs (15 000−16 000 h^{-1}) in small scale (several g-polymer scale) as well as in large scale polymerization (70 g-polymer scale) (entries 9 and 10).

In the ^{1}H NMR studies of the reaction between **15** and PO, a set of signals indicating a protonated version of the spiro-Meisenheimer anion 2,4-$(NO_2)_2C_6H_3$−OCH_2CH-(Me)OH and 2,4-$(NO_2)_2C_6H_3$−$OCH(Me)CH_2OH$ is observed at the initial stage (10 min). After 30 min, signals representing both a spiro-Meisenheimer anion and its protonated version are observed. After 1 h, the integration ratio of [spiro-Meisenheimer anion + its protonated compound]/[DNP] is 1.6. At 2 h, the ratio reaches ∼2.0. At a reaction time of 4 h, the ratio remains at a value of ∼2.0. Since 2,4-dinitrophenol does not react with PO at room temperature, we presume that 2,4-$(NO_2)_2C_6H_3$−$OCH_2CH(Me)OH$ and 2,4-$(NO_2)_2C_6H_3$−$OCH(Me)$-CH_2OH are generated through the protonation of the spiro-Meisenheimer anion or the alkoxide. The rate of PO attack is not altered in the presence of 50 equivalents of water. This contrasts with the rate of **10**, which is significantly reduced in the presence of 50 equivalents of water. In fact, **10** does not generate **14** even after a 4 h reaction (Figure 9).

Summary and Discussion

Cobalt(III) complexes, prepared from salen-type ligands bearing four quaternary ammonium salt units, can adopt an unusual binding mode that differs from that of a conventional salen−Co(III) complex. Imine donors in salen-type ligand do not coordinate with cobalt. Instead, DNPs, which counter the quaternary ammonium cation, coordinate with cobalt creating a cobaltate complex with a formal negative charge on cobalt. This is supported by ^{1}H, ^{13}C, and ^{15}N NMR spectroscopy, IR spectroscopy, DFT calculations, and cyclic voltammetric (CV) studies. Adoption of such an unusual binding mode is allowed when the substituent on the 3-position of salicylaldehyde in the salen-type ligand is not bulky (**3**, **7**, and **10** in Chart 1). Salen-type ligands, prepared from either salicylaldehyde containing a bulky *tert*-butyl substituent on the 3-position or $H_2NCMe_2CMe_2$-NH_2, afford complexes of a conventional imine-coordinated binding mode (**4**, **8**, and **11** in Chart 1). Unusual uncoordinated imine complexes show extraordinarily high activities, while those of a conventional imine-coordinated structure show relatively low or negligible activities in CO_2/PO copolymerization.

The status of DNPs in uncoordinated imine complexes depends on the solvent, ligand structure, and temperature. In THF, whose medium effect resembles that of the polymerization medium, the two DNPs are situated in a coordinated state, while the other two are scrambling between a coordinated and

(23) In previous report (ref 2), we mistakenly used 60 mol % NaDNP in preparation of **5**.

(24) Shan, S.-o.; Loh, S.; Herschlag, D. *Science* **1996**, *272*, 97.
(25) (a) Barnes, J. C.; Weakley, T. J. R. *Acta Crystallogr.* **2003**, *E59*, m160. (b) Paola, G. P.; Bertolasi, V.; Ferretti, V.; Gilli, V. *J. Am. Chem. Sec.* **1994**, *116*, 909.
(26) Magonski, J.; Pawlak, Z.; Jasinski, T. *J. Chem. Soc., Faraday Trans.* **1993**, *89*, 119.

a uncoordinated state. It was documented that neutral diamagnetic octahedral cobalt(III) complexes remain very inert in regard to ligand substitution reactions.[27] However, for uncoordinated imine cobaltate complexes, cobalt possesses a negative charge in order to expel the negatively charged ligand, which cannot move far from the cobalt center due to ion−ion interactions with a quaternary ammonium cation. The uncoordinated negatively charged anion is thermodynamically unstable and prone to recoordinating to the cobalt center. Balancing between these two statuses results in scrambling. Some tetradentate cobaltate(III) complexes bearing a −1 charge on cobalt have been previously reported.[28] They are also prone to interconversion between four-, five-, and six-coordinate states in the presence of additional neutral or anionic ligands.[29,15a] The extraordinarily high activities may be attributed to the scrambling of the negatively charged ligand. Equation 4 shows a plausible chain-growing mechanism for CO_2/PO copolymerization. In this mechanism, a key step is the nucleophilic attack of the terminal carbonate anion on a coordinated epoxide. A facile back-side attack is easily allowed, if the carbonate anion is able to scramble between a coordinated and a uncoordinated state.[30]

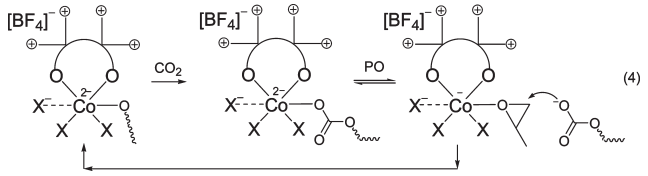

(4)

The binding affinity of the two fluxional DNPs is sensitive to the ligand structure (**7** > **10** > **3**). In addition, it may influence catalytic activity in that the more loosely DNP binds cobalt, the higher the activity. A more loosely bound status can be attained by employing the $[DNP\cdots H\cdots DNP]^-$ homoconjugation instead of the fluxional DNPs, as in **15** (Chart 2). Complex **15** has two coordinated DNPs and two loosely bound $[DNP\cdots H\cdots DNP]$ anions, providing ∼1.5 times higher activity than **10**, which has four DNP anions. Another advantage of **15** is that it is not so sensitive to water impurity and, therefore, consistently provides an excellent polymerization activity (TOF 1.5×10^3 h^{-1}) at both small (10 g PO scale) and large scale (230 g PO scale) polymerizations. Induction times are below 1 h, even when PO is dried with molecular sieves and a sacrificial drying agent such as CaH_2 is not used.

Complexes with four DNPs such as **3** and **10** show fluctuating induction times (1−10 h), depending on the dryness of the polymerization system. It is observed in the ^1H NMR studies with **10** that the rate of DNP attack on PO is diminished by a certain amount of water. We guess that stabilization of uncoordinated DNPs by hydrogen bonding with water is responsible for the decrease in reaction rate. It may be suggested that the slower rate is due to competitive coordination of water with the cobalt center, which consequently hampers the PO coordination. However, water and epoxide reportedly bind with similar affinity to the cobalt center of a salen−Co(III) complex.[31] The $[DNP\cdots H\cdots DNP]^-$ homoconjugation is not as hygroscopic as pure DNP^-, and hence, the catalytic performance of **15** is not as highly affected by water impurity as is **10**. Variations in the induction time of **10** are minimized by use of **14**, which is prepared by reacting a high concentration of **10** with/in PO for 1 h, such that the ratio of [residual water in PO]/[**10**] is negligible.

Acknowledgment. This work was supported by the Korea Research Foundation Grant funded by the Korean Government (MOEHRD, Basic Research Promotion Fund) (KRF-2008-314- C00186).

Supporting Information Available: Synthetic details and characterization data for all new compounds, polymerization procedures, and NMR spectra. This material is available free of charge via the Internet at http://pubs.acs.org.

(27) Becker, C. A. L.; Motladiile, S. *Synth. React. Inorg. Met.-Org. Chem.* **2001**, *31*, 1545.
(28) (a) Collins, T. J.; Richmond, T. G.; Santarsiero, B. D.; Treco, B. G. R. T. *J. Am. Chem. Soc.* **1986**, *108*, 2088. (b) Gray, H. B.; Billig, E. *J. Am. Chem. Soc.* **1963**, *85*, 2019.
(29) Langford, C. H.; Billig, E.; Shupack, S. I.; Gray, H. B. *J. Am. Chem. Soc.* **1964**, *86*, 2958.
(30) For (salen)Cr-based binary system, it was proposed that the chain propagation step proceeds via a concerted insertion of epoxide into a metal-bound carbonate, but in another DFT study, a bimolecular process in which a metal-bound carbonate attacks a metal-bound epoxide was suggested. See: (a) Darensbourg, D. J.; Yarbrough, J. C. *J. Am. Chem. Soc.* **2002**, *124*, 6335. (b) Luinstra, G. A.; Haas, G. R.; Molnar, F.; Bernhart, V.; Eberhardt, R.; Rieger, B. *Chem.—Eur. J.* **2005**, *11*, 6298.
(31) Nielsen, L. P. C.; Stevenson, C. P.; Blackmond, D. G.; Jacobsen, E. N. *J. Am. Chem. Soc.* **2004**, *126*, 1360.